

ANL/CMT/CP-102089

**From Gems to Lithium Battery Electrodes:  
The Significance of the Diamond, Ruby (Sapphire),  
Spinel and Peridot Structures**

**RECEIVED**

by

**JUL 10 2000**

**OSTI**

**Michael M. Thackeray  
Argonne National Laboratory  
Chemical Technology Division  
Electrochemical Technology Program  
Argonne, IL 60439**

The submitted manuscript has been created by the University of Chicago as Operator of Argonne National Laboratory ("Argonne") under Contract No. W-31-109-ENG-38 with the U.S. Department of Energy. The U.S. Government retains for itself, and others acting on its behalf, a paid-up, nonexclusive, irrevocable worldwide license in said article to reproduce, prepare derivative works, distribute copies to the public, and perform publicly and display publicly, by or on behalf of the Government.

**May 2000**

**To be presented at the 10th International Meeting on Lithium Batteries, Como, Italy,  
May 28-June 2, 2000**

## **DISCLAIMER**

**Portions of this document may be illegible  
in electronic image products. Images are  
produced from the best available original  
document.**

## **DISCLAIMER**

This report was prepared as an account of work sponsored by an agency of the United States Government. Neither the United States Government nor any agency thereof, nor any of their employees, make any warranty, express or implied, or assumes any legal liability or responsibility for the accuracy, completeness, or usefulness of any information, apparatus, product, or process disclosed, or represents that its use would not infringe privately owned rights. Reference herein to any specific commercial product, process, or service by trade name, trademark, manufacturer, or otherwise does not necessarily constitute or imply its endorsement, recommendation, or favoring by the United States Government or any agency thereof. The views and opinions of authors expressed herein do not necessarily state or reflect those of the United States Government or any agency thereof.

**From Gems to Lithium Battery Electrodes: The Significance of the  
Diamond, Ruby (Sapphire), Spinel and Peridot Structures**

Michael M. Thackeray

Electrochemical Technology Program, Chemical Technology Division

Argonne National Laboratory, Argonne, Illinois 60439, USA

**Abstract**

The materials used for the negative and positive electrodes of rechargeable "lithium-ion" batteries have host structures that can accommodate and release lithium over a wide compositional range. In these batteries, carbon and intermetallic compounds have been widely exploited as the negative electrodes, and transition metal oxides as the positive electrodes. For a lithium-ion battery to perform adequately, the structural integrity of the electrode host structures must be maintained throughout discharge and charge for many hundreds of cycles. Nature provides many examples of stable compounds that can be produced under variable conditions of temperature and pressure. As such, the mineral world can be used as a guide for the selection of materials in technological applications. This paper highlights the structural relationships that exist between precious and semi-precious gems such as diamond, ruby (sapphire), spinel and peridot and insertion electrodes for lithium batteries.

**Introduction**

Lithium-ion batteries operate by an electrochemical reaction during which lithium ions are extracted from one host electrode structure and inserted into another with concomitant oxidation and reduction occurring at the two electrodes, respectively. In order to achieve high electrode capacities and good cycle life, as much lithium as possible must be inserted into and

extracted from the electrodes during charge and discharge without damaging the integrity of the host electrode structures. This requirement puts a heavy emphasis on the need to use (1) host structures that are stable to lithium insertion/extraction over a wide compositional range and (2) transition metal ions that at full charge and discharge have stable oxidation states. Lithium insertion and extraction reactions with stable host structures at room temperature tend to form metastable products. Therefore, it can be anticipated that greater stability of the lithiated and delithiated structures will lead to enhanced cycle life. In general, structural stability will be more readily maintained with cubic structures that "breathe" isotropically on lithium insertion with minimal change to the  $\alpha$  lattice parameter and unit cell volume. This immediately implies that host electrodes with "simple" high symmetry structures are more likely to provide the required structural stability than low symmetry structures. From a crystallographic standpoint, high-symmetry host structures provide many symmetrically equivalent sites for lithium. Crystallographically equivalent sites are energetically equivalent; they facilitate fast lithium-ion transport, provided that the activation energy for lithium transport from site to site is low.

The mineral world provides numerous examples of stable compounds and structure types that are produced under various conditions, such as at high temperature or high pressure, from a melt or solution, from a solid-state reaction, or by ion exchange. This large family of stable structures can thus be used as a guide for selecting materials for technological applications such as host electrode structures for lithium batteries. This will be particularly true if structure types that exist in nature correspond to the structures of the fully lithiated, partially lithiated and fully delithiated electrodes. This paper highlights the structural relationships between various minerals and insertion electrodes for lithium batteries.

## Structural Properties of Gemstones and Lithium Battery Electrodes

Table 1 shows a list of selected precious and semi-precious gemstones, ranked according to the Mohr hardness scale. The "precious" gems of diamond and the corundum family (ruby and sapphire) are the hardest known materials, both of which have simple structures. The diamond structure consists of two interlinked face-centered-cubic (carbon) arrays (space group Fd-3m), whereas the corundum structure ( $\alpha$ -Al<sub>2</sub>O<sub>3</sub>) has rhombohedral symmetry (R-3c) with a hexagonal-close-packed oxygen array. The mineral "spinel" (MgAl<sub>2</sub>O<sub>4</sub>), which is a "semi-precious" gem, has cubic symmetry (space group Fd-3m) and a cubic-close-packed oxygen array. At the other extreme of the Mohr hardness scale are other "simple" structures such as that of periclase (MgO, rock-salt-type structure), fluorite (CaF<sub>2</sub>, fluorite-type structure), and sphalerite (ZnS, zinc-blende-type structure), all of which have cubic-close-packed anion or cation arrays.

Many minerals consist of silicates and alumino-silicates; they include the beryl family (e.g., emerald and aquamarine, Al<sub>2</sub>Be<sub>3</sub>Si<sub>6</sub>O<sub>18</sub>), the quartz family (e.g., amethyst and citrine,  $\alpha$ -SiO<sub>2</sub>) and spodumene (LiAl[Si<sub>2</sub>O<sub>6</sub>]). These minerals tend to have more complex framework structures in which the oxygen ions deviate markedly from close packing; their structure types are not common as host electrodes for lithium. Exceptions to this general rule exist, such as in peridot (Mg<sub>2-x</sub>Fe<sub>x</sub>SiO<sub>4</sub>) with a hexagonally-close-packed olivine-type structure.

Most transition metal oxides, MO<sub>x</sub>, that are of major interest as insertion electrodes for lithium batteries have close-packed oxygen arrays in which the M cations occupy octahedral sites [1]. The MO<sub>x</sub> framework can accommodate lithium up to the rock-salt composition at which the total number of cations equals the number of anions. In cubic-close-packed structures such as layered-type LiCoO<sub>2</sub>, LiNiO<sub>2</sub> and Li<sub>1.2</sub>V<sub>3</sub>O<sub>8</sub>, and spinel-type LiMn<sub>2</sub>O<sub>4</sub> and Li<sub>4</sub>Ti<sub>5</sub>O<sub>12</sub>, the

**Table 1. A selected list of precious and semi-precious gems**

Name of Gem	Structure Type	Crystal Symmetry	Composition	Mohr Hardness
Diamond	Diamond	Cubic	C	10
Ruby, Sapphire	Corundum	Rhombohedral	$\text{Al}_2\text{O}_3$	9
Spinel	Spinel	Cubic	$\text{MgAl}_2\text{O}_4$	8
Emerald, Aquamarine	Beryl	Hexagonal	$\text{Al}_2\text{Be}_3\text{Si}_6\text{O}_{18}$	7.5 – 8
Amethyst, Citrine	Alpha-Quartz	Hexagonal	$\text{SiO}_2$	7
Spodumene	Spodumene	Monoclinic	$\text{LiAl}(\text{Si}_2\text{O}_6)$	6.5 – 7
Peridot	Olivine	Orthorhombic	$(\text{Mg}_{2-x}\text{Fe}_x)\text{SiO}_4$	6.5 – 7
Periclase	Rock-salt	Cubic	$\text{MgO}$	5.5 – 6
Fluorspar	Fluorite	Cubic	$\text{CaF}_2$	4
Sphalerite	Zinc Blende (Diamond)	Cubic	$\text{ZnS}$	3.5 – 4

$\text{CoO}_2$ ,  $\text{NiO}_2$ ,  $\text{V}_3\text{O}_8$ ,  $[\text{Mn}_2]\text{O}_4$  and  $[\text{Ti}_5\text{Li}]\text{O}_{12}$  frameworks are stable to lithium insertion and extraction over a wide compositional range. By contrast, hexagonal close-packed structures are unstable to lithium insertion as the composition approaches the rock-salt stoichiometry; they shear toward cubic-close-packing because of increasing electrostatic interactions between the incoming lithium ions and transition metal ions in neighboring face-shared octahedral sites. Lithium ions can reside comfortably in either tetrahedral or octahedral sites of the  $\text{MO}_x$  host structure; what type of site is occupied by lithium during the electrochemical reaction strongly depends on the cation arrangement in the host and on the lithium content. Lithium diffusion in a cubic-close-packed structure such as  $\text{Li}_x\text{CoO}_2$  is fast, because all the octahedral sites occupied by lithium are crystallographically (energetically) equivalent and because the activation energy to pass through a neighboring face-shared tetrahedral site is low.

## Transition metal oxide positive electrodes

### 1. $Fe_3O_4$ and $\alpha$ - $Fe_2O_3$ – spinel and ruby/sapphire (corundum-type) structures

Iron oxides such as  $Fe_3O_4$  (magnetite, spinel-type structure) and  $\alpha$ - $Fe_2O_3$  (hematite, corundum-type (ruby/sapphire) structure) were investigated in the early 1980's as positive electrodes for high temperature lithium cells [2, 3]. For example, Godshall et al. reported the equilibrium potential profile of a  $LiAl/LiCl, KCl/Li_xFe_3O_4$  high temperature cell [3]. The voltage vs. capacity plot shows several discrete voltage plateaus, each plateau corresponding to a multi-phase reaction at the  $Li_xFe_3O_4$  electrode. The reaction occurs by lithium insertion into a cubic-close-packed oxygen array and concomitant reduction and extrusion of iron from the structure. The change in Li:Fe ratio in the electrode during discharge gives rise to several discrete structure types: 1)  $Fe_3O_4$  (spinel), 2)  $LiFe_5O_8$  (spinel), 3)  $LiFeO_2$  (rock salt), and 4)  $Li_2O$  (antifluorite). These reaction products have simple, cubic structures that exist in the mineral world (Table 1); they are stable at 400 °C and also at room temperature. What is remarkable about this reaction is that the oxygen array remains cubic-close-packed throughout discharge; the reaction simply involves diffusion of lithium and iron ions into and out of a stable network of tetrahedra and octahedra. Moreover, at 400 °C, all the reaction processes are reversible despite the extrusion of metallic iron from the structure. This reaction provides an excellent example of how stable structure types play a key role in determining the cycling behavior of electrochemical cells.

Lithium insertion into  $\alpha$ - $Fe_2O_3$  with the corundum-type structure exhibited by ruby and sapphire causes a shear of the hexagonal close-packed oxygen layers to cubic-close-packing in response to increased electrostatic interactions between the incoming lithium ions and the iron ions in neighboring face-shared octahedral sites as described earlier; this shearing induces a phase transition to a  $\gamma$ - $Li_8Fe_2O_3$  defect-spinel-type structure. Thereafter, the reaction path

follows a reaction sequence similar to that given for  $\text{Li}_x\text{Fe}_3\text{O}_4$  above [2]. The transition from  $\alpha\text{-Fe}_2\text{O}_3$  to  $\gamma\text{-Li}_8\text{Fe}_2\text{O}_3$  highlights the greater stability of cubic-close-packed electrode structures over hexagonal-close-packed structures to lithium insertion.

#### *$\text{LiMn}_2\text{O}_4$ – the spinel structure*

The lithium spinels,  $\text{LiB}_2\text{O}_4$ , are of much greater interest to the battery industry than the iron oxide spinels because the  $[\text{B}_2]\text{O}_4$  spinel framework provides an uninterrupted three-dimensional interstitial space for  $\text{Li}^+$ -ion transport at room temperature over a wide compositional range of  $x$  in  $\text{Li}_x[\text{B}_2]\text{O}_4$ . Many papers have been written on spinel electrodes [1, 4]. Of the spinels,  $\text{LiMn}_2\text{O}_4$  is a particularly attractive electrode material. The  $[\text{Mn}_2]\text{O}_4$  spinel framework remains intact over the complete range of  $x$  in  $\text{Li}_x\text{Mn}_2\text{O}_4$ , as shown in schematic illustrations of the structures for  $\lambda\text{-MnO}_2$  ( $[\text{Mn}_2]\text{O}_4$ ,  $x=0$ ),  $\text{LiMn}_2\text{O}_4$  ( $x=1$ ) and  $\text{Li}_2\text{Mn}_2\text{O}_4$  ( $x=2$ ) (Fig. 1a-c). The stability of the many spinel compounds found in nature (they are regarded as “line phases”) can be understood from the electrochemical and structural properties of spinels to lithium insertion and extraction. Because the interstitial space of a stoichiometric  $\text{A}[\text{B}_2]\text{O}_4$  spinel structure is not energetically favorable for  $\text{Li}^+$ -ion occupation, lithium insertion induces an immediate first-order transition during which the tetrahedral site (A) cations are displaced into neighboring octahedral sites to generate an ordered rock-salt phase  $\text{LiA}[\text{B}_2]\text{O}_4$ . For  $\text{Li/Li}_x\text{Mn}_2\text{O}_4$  electrochemical cells, lithium insertion occurs at approximately 3 V vs. Li for the range  $1 \leq x \leq 2$ . On the other hand, considerable energy is required to destabilize the spinel by removing lithium ions from the tetrahedral sites of  $\text{LiMn}_2\text{O}_4$ , as reflected by the high voltage of  $\text{Li/Li}_x\text{Mn}_2\text{O}_4$  cells (4 V) over the range  $0 < x \leq 1$ . Therefore, the lithium insertion and extraction reactions both emphasize the stability of the stoichiometric  $\text{LiMn}_2\text{O}_4$  spinel composition. From a structural standpoint, the  $\text{Li}_x\text{Mn}_2\text{O}_4$  system is strongly connected to the mineral world. Lithium insertion

into  $\text{LiMn}_2\text{O}_4$  ( $\text{Mn}^{4+/3+}$ ) results in  $\text{Li}_2[\text{Mn}_2]\text{O}_4$  ( $\text{Mn}^{3+}$ ) with an ordered rock-salt/periclase-type structure; complete extraction of lithium from the spinel structure results in  $\lambda\text{-MnO}_2$  ( $\text{Mn}^{4+}$ ) with the structure type of the mineral atacamite  $\text{Cu}_2(\text{OH})_3\text{Cl}$  [5] (see Fig. 2a-c). The stability of the  $\text{Mn}_2\text{O}_4$  spinel framework to lithium insertion and extraction and the fact that both  $\text{Mn}^{4+}$  and  $\text{Mn}^{3+}$  are stable in mineral forms, such as  $\beta\text{-MnO}_2$  (pyrolusite) and  $\text{Mn}_2\text{O}_3$  (bixbyite), augers well for the future of  $\text{Li}_x\text{Mn}_2\text{O}_4$  spinel electrodes in commercial Li-ion cells, particularly when used over the high-voltage (4 V) range; over this range, the cubic symmetry of the spinel framework is maintained with a relatively small change to the unit cell volume (~6%). Such crystallographic stability and structural relationships to minerals do not hold for other high-voltage lithium battery electrodes such as  $\text{Li}_x\text{CoO}_2$  and  $\text{Li}_x\text{NiO}_2$  ( $0 \leq x \leq 1$ ).

#### *$\text{LiFePO}_4$ – the peridot (olivine-type) structure*

It was recently demonstrated that the  $\text{FePO}_4$  framework of  $\text{LiFePO}_4$  can provide a host structure for lithium [6].  $\text{LiFePO}_4$  is isostructural with the mineral peridot,  $\text{Mg}_{2-x}\text{Fe}_x\text{SiO}_4$ , in which the P atoms of the olivine-type structure substitute for the Si atoms and the Li and Fe atoms for Mg and Fe. Both olivine (hexagonal-close-packed) and spinel (cubic-close-packed) structures have the general formula  $\text{AB}_2\text{O}_4$ , in which the A cations occupy tetrahedral sites and the B cations octahedral sites; the difference in oxygen packing leads to different cation arrangements in the two structure types. In peridot, the Mg and Fe ions occupy one-half of the available octahedral sites and the Si ions one-eighth of the tetrahedral sites. In "spinel",  $\text{MgAl}_2\text{O}_4$ , the Al ions occupy one-half of the octahedral sites and the Mg ions one-eighth of the tetrahedral sites of a cubic-close-packed oxygen array.

An illustration of the  $\text{LiFePO}_4$  olivine structure is shown in Fig. 2a. The structure may be regarded as layered; it has layers of  $\text{Fe}^{2+}$  and  $\text{P}^{5+}$  ions that alternate with layers of  $\text{Li}^+$  ions in a

direction perpendicular to the close-packed oxygens. The Fe-P layers consist of alternating columns of isolated  $\text{PO}_4$  tetrahedra and edge-shared  $\text{FeO}_6$  octahedra. The  $\text{PO}_4$  tetrahedra are connected to one another in their columns by interstitial octahedra. These octahedra share four of their eight faces with two occupied P tetrahedra and two Li octahedra. In the lithium layers of the  $\text{LiFePO}_4$  structure, one-half of the octahedral sites are occupied by the  $\text{Li}^+$  ions; the remaining interstitial octahedra share three faces with occupied polyhedra, one with a P tetrahedron and two with Li octahedra. Thus, in the olivine structure there are two crystallographically independent sets of interstitial octahedral sites. Both sets are energetically unfavorable for additional Li occupation because they share several faces with neighboring, occupied polyhedra. In  $\text{Mg}_{2-x}\text{Fe}_x\text{SiO}_4$ , the Mg and Fe ions can partially substitute for one another on the two sets of octahedral sites. In  $\text{LiFePO}_4$ , it is also possible for the  $\text{Li}^+$  and  $\text{Fe}^{2+}$  ions to partially substitute for one another. In such an instance, any  $\text{Fe}^{2+}$  ions within the lithium layers would reduce not only the  $\text{Li}^+$ -ion conductivity but also reduce the ease with which it is possible to extract all the lithium from the structure; this limitation makes it difficult to obtain an electrode capacity close to the theoretical value (170 mAh/g). Therefore, processing conditions must be carefully controlled to ensure that a structure as close to the ideal layered configuration is achieved.

Lithium extraction from  $\text{LiFePO}_4$  is accompanied by the concomitant oxidation of  $\text{Fe}^{2+}$  ions to  $\text{Fe}^{3+}$  to yield the ideal  $\text{FePO}_4$  host framework (Fig. 2b). This reaction is analogous to the extraction of lithium from the spinel  $\text{LiMn}_2\text{O}_4$  during which the  $\text{Mn}^{3+}$  ions are oxidized to yield  $\lambda\text{-MnO}_2$ . However, unlike  $\text{LiMn}_2\text{O}_4$ , which can be reduced by lithium insertion to yield the rock-salt phase  $\text{Li}_2\text{Mn}_2\text{O}_4$ , lithium insertion into the  $\text{LiFePO}_4$  is not possible without major structural changes. First, lithium insertion into  $\text{LiFePO}_4$  would necessitate the reduction of the

$\text{Fe}^{2+}$  ions and the extrusion of metallic iron from the oxygen array; it is most unlikely that such a reaction would be highly reversible at room temperature. Second, the interstitial octahedral sites located in the columns of  $\text{PO}_4$  tetrahedra and in the lithium layer of the  $\text{LiFePO}_4$  structure are not energetically favorable for Li occupation, as described above. Therefore, from a structural viewpoint, the  $\text{B}_2\text{O}_4$  framework of  $\text{Li}_x[\text{B}_2]\text{O}_4$  spinels is significantly more attractive as a host structure for lithium than its olivine counterpart because it provides 1) a more energetically favorable interstitial space for lithium-ion diffusion, 2) a greater structural stability over a wider compositional range of  $x$ , and 3) a superior theoretical electrode capacity ( $x_{\text{max}}=2$  for spinel and  $x_{\text{max}}=1$  for olivine).

### **Intermetallic negative electrodes**

#### *InSb – the sphalerite/zinc-blende (diamond-type) structure*

Intermetallic electrodes have been investigated extensively as negative electrodes for lithium batteries [7, 8]. Because metals have dense structures, their reactions with lithium tend to lead to displacement reactions in which new  $\text{Li}_x\text{M}$  phases are formed with large changes in crystallographic volume. Such phenomena are well known for the binary systems  $\text{Li}_x\text{Al}$ ,  $\text{Li}_x\text{Si}$  and  $\text{Li}_x\text{Sn}$ . The recent announcement that certain intermetallic systems such as  $\text{Cu}_6\text{Sn}_5$  and InSb might accommodate lithium with relatively small changes in crystallographic volume has prompted detailed investigations of  $\text{Li}_x\text{MM}'$  structures in which the M and M' atoms provide a zinc-blende host framework (diamond network) for lithium atoms [9, 10].

The  $\text{Cu}_6\text{Sn}_5$  structure is related to that of nickel arsenide,  $\text{NiAs}$ , as shown in a [001] projection of the structure in Fig. 3a. Lithium insertion into  $\text{Cu}_6\text{Sn}_5$  induces a displacement of 50% of the Sn atoms to yield a lithiated zinc-blende-type structure resembling  $\text{Li}_2\text{CuSn}$ , in which the Cu and Sn atoms form a diamond network, as shown in Fig. 3b. This reaction, which results

in a 59% volume expansion of the host structure, is reversible and has considerable hysteresis [9]. Nevertheless, the existence of stable compounds  $\text{Li}_x\text{MM}'$ , such as  $\text{Li}_2\text{CuSn}$ , has immediate implications for designing intermetallic host electrode structures with a stable zinc-blende framework  $\text{MM}'$  that can accommodate lithium over a wide compositional range with a relatively small isotropic change to the unit cell volume. The zinc-blende framework, shown schematically in Fig. 3c, has a diamond-type arrangement of atoms with a three-dimensional interstitial space of intersecting hexagonal channels; in the fully lithiated structure  $\text{Li}_2\text{MM}'$ , as typified by  $\text{Li}_2\text{CuSn}$  (Fig. 3b), the lithium atoms occupy two crystallographically independent sites in the hexagonal channels. In this respect,  $\text{Li}_2\text{CuSn}$  is a fully saturated intermetallic structure, in much the same way as the rock-salt phase  $\text{Li}_2\text{Mn}_2\text{O}_4$  represents a fully saturated transition metal oxide structure, i.e., both compounds have structures beyond which no further Li atoms can be accommodated without major structural rearrangements.

Recent studies of the small band-gap semiconductor InSb have provided evidence that the zinc-blende framework of InSb can be tailored to provide a possible host structure for lithium [10]. After one “break-in” cycle,  $\text{Li}/\text{Li}_x\text{InSb}$  cells provide excellent electrochemical reversibility. Powder X-ray diffraction and EXAFS data of cycled  $\text{Li}_x\text{InSb}$  electrodes and theoretical structure calculations of  $\text{Li}_x\text{InSb}$  compounds [11] indicate that a modified  $\text{Li}_x\text{In}_{1-x}\text{Sb}$  zinc-blende framework is formed, which is more tolerant to the reversible uptake of lithium than the parent InSb structure. Of particular significance is that the fully lithiated product, assuming complete replacement of In by Li and complete occupation of the interstitial sites by lithium, is  $\text{Li}_3\text{Sb}$ , which has a cubic unit cell only 5.6% larger than that of InSb [10]. For the InSb to  $\text{Li}_3\text{Sb}$  transition, the cubic-close-packed Sb array of the zinc-blende framework remains intact (note that this reaction is similar to that described earlier for magnetite,  $\text{Fe}_3\text{O}_4$ , in which the oxygen

array provides a stable framework for lithium insertion/iron extrusion [2]). In practice, not all the In is extruded from the InSb lattice. Powder X-ray diffraction data of cycled electrodes are consistent with the presence of a  $\text{Li}_x\text{In}_{1-x}\text{Sb}$  zinc-blende-type framework at the top of charge (1.2 V vs. Li) and at the end of discharge (0.5 V vs. Li) of  $\text{Li}/\text{Li}_x\text{InSb}$  cells. Studies are in progress to elucidate the exact reaction mechanism that takes place and to determine whether a lithiated structure " $\text{Li}_{2+x}\text{In}_{1-x}\text{Sb}$ " that is isostructural with  $\text{Li}_2\text{CuSn}$  exists as an intermediate between the parent InSb and fully lithiated  $\text{Li}_3\text{Sb}$ . These early data hold exciting prospects for fabricating an intermetallic host framework that is stable to lithium insertion and extraction over a wide compositional range with a relatively small change in unit cell volume. Such a host "insertion" electrode, based on a diamond network of atoms, would contrast strongly with conventional intermetallic electrodes that operate by multi-phase displacement reactions involving large changes in crystallographic volume.

### **Conclusions**

The stability of host electrode structures when accommodating lithium plays a key role in determining the cycle-life of lithium batteries. As such, minerals can provide a guide for the selection of electrode materials that can accommodate as much lithium as possible without compromising structural stability. From this viewpoint, the *spinel* system  $\text{Li}_x[\text{Mn}_2]\text{O}_4$ , which is of interest as a positive electrode, is strongly connected to the mineral world, forming an *atacamite*-type structure on full charge ( $x=0$ ), a stoichiometric *spinel* structure at  $x=1$ , and a *rock-salt/periclase* phase on complete discharge ( $x=2$ ). The *zinc-blende* structure with its *diamond* network of atoms holds promise for generating a new class of intermetallic host structures as negative electrodes for lithium batteries.

## Acknowledgments

Grateful thanks are expressed to my colleagues at CSIR, South Africa; Oxford University; UK and Argonne National Laboratory, USA, who contributed over the years to much of the information reported in this paper. Particular thanks go to J.T. Vaughey for preparing the computer illustrations of the structures. Financial support for writing this article from the Chemical Sciences Division of the Office of Basic Energy Sciences, Department of Energy under contract No. W31-109-Eng-38 is gratefully acknowledged.

## References

1. M. M. Thackeray, in *Handbook of Battery Materials* (Ed. J. O. Besenhard), Wiley-VCH, Wienheim, Germany, Part III.1, p. 293 (1999).
2. M. M. Thackeray, W. I. F. David and J. B. Goodenough, *J. Solid State Chem.*, 55 (1984) 280.
3. N. A. Godshall, I. D. Raistrick and R. A. Huggins, *J. Electrochem. Soc.*, 131 (1984) 543.
4. M. M. Thackeray, *Prog. in Solid State Chem.*, 25 (1997) 1.
5. A. F. Wells, in: *Structural Inorganic Chemistry*, (4<sup>th</sup> Edition), Clarendon Press, Oxford, Ch. 4, p. 143 (1975).
6. K. S. Nanjundaswamy, A. K. Pahdi, J. B. Goodenough, S. Okada, H. Ohtsuka, H. Arai and J. Yamaki, *Solid State Ionics*, 3 (1996) 178.
7. R. A. Huggins, in *Handbook of Battery Materials* (Ed. J. O. Besenhard), Wiley-VCH, Wienheim, Germany, Part III.4, p. 359 (1999).
8. M. Winter, J. O. Besenhard, M. E. Spahr and P. Novak, *Adv. Mater.*, 10 (1998) 725.
9. K. D. Kepler, J. T. Vaughey, and M. M. Thackeray, *Electrochem. and Solid-State Lett.*, 2 (1999) 307.

10. J. T. Vaughey, J. O'Hara and M. M. Thackeray, *Electrochem. and Solid-State Lett.*, 3 (2000)

13.

11. C. S. Johnson, J. T. Vaughey, J. Kropf, H. Tostmann, R. Benedek and M. M. Thackeray,

unpublished data.

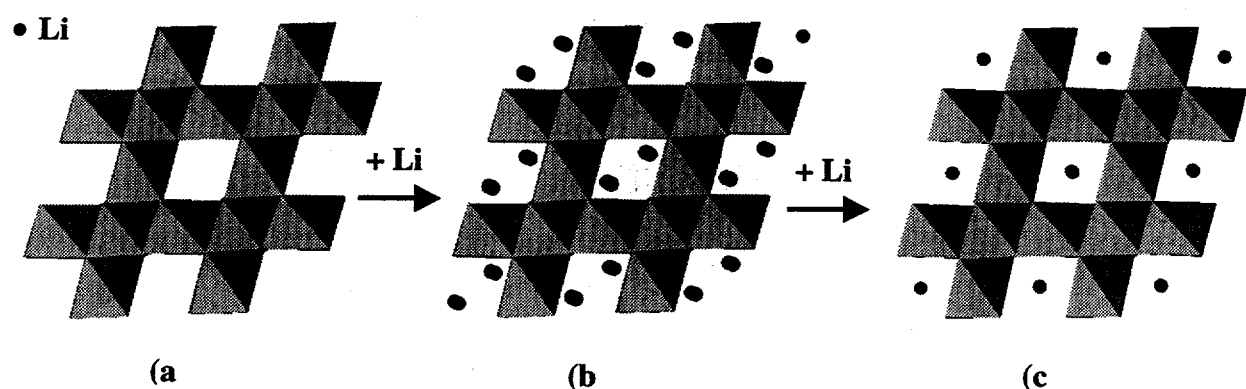
### **Captions to Table and Figures**

Table 1. A selected list of precious and semi-precious gems.

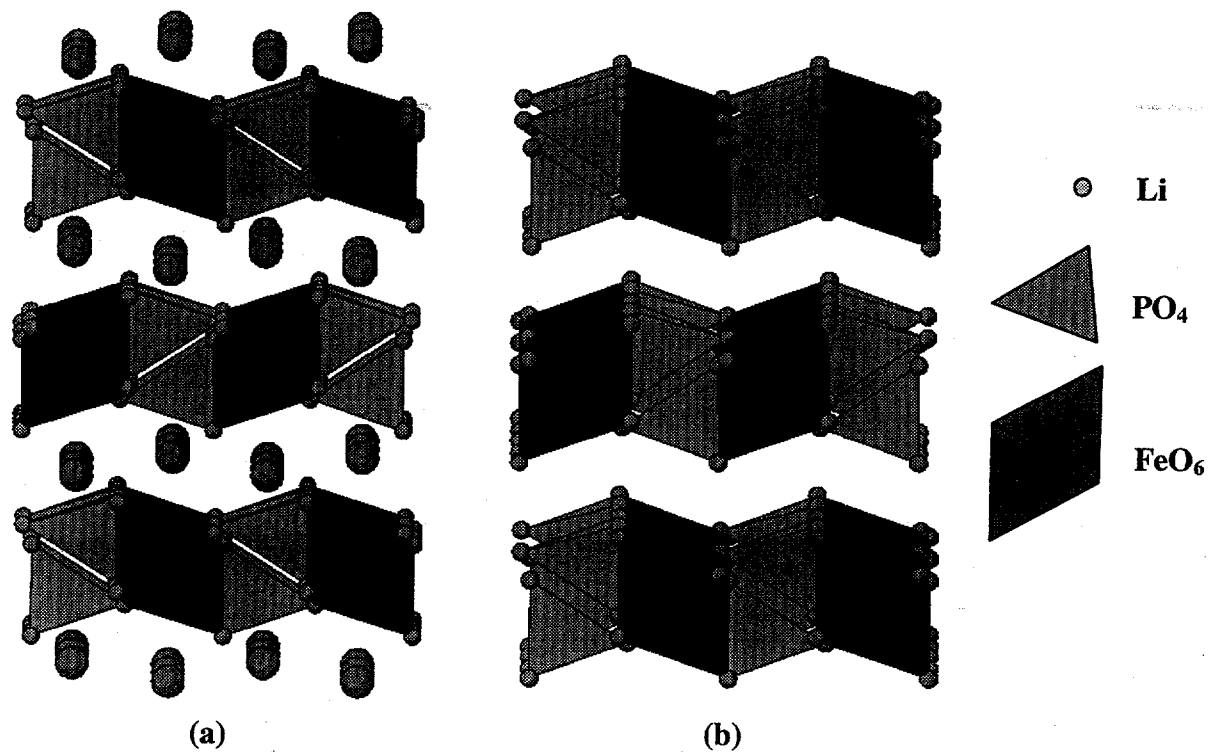
Figure 1. Schematic illustrations of  $\text{Li}_x\text{Mn}_2\text{O}_4$  structures with related mineral forms, a)  $\lambda$ - $\text{MnO}_2$  ( $x=0$ ), atacamite –  $\text{Cu}_2(\text{OH})_3\text{Cl}$ ; b)  $\text{LiMn}_2\text{O}_4$  ( $x=1$ ), spinel –  $\text{MgAl}_2\text{O}_4$ ; c)  $\text{Li}_2\text{Mn}_2\text{O}_4$  ( $x=2$ ), (ordered) rock salt –  $\text{NaCl}$ , periclase –  $\text{MgO}$ .

Figure 2. The structures of a)  $\text{LiFePO}_4$  (olivine), and b) the  $\text{FePO}_4$  olivine framework.

Figure 3. Crystallographic projections of a) the NiAs ("CuSn") framework of  $\text{Cu}_6\text{Sn}_5$ , b)  $\text{Li}_2\text{CuSn}$ , and c) the zinc-blende ("CuSn") framework of  $\text{Li}_2\text{CuSn}$  with a diamond-type lattice.



**Figure 1**



**Figure 2**

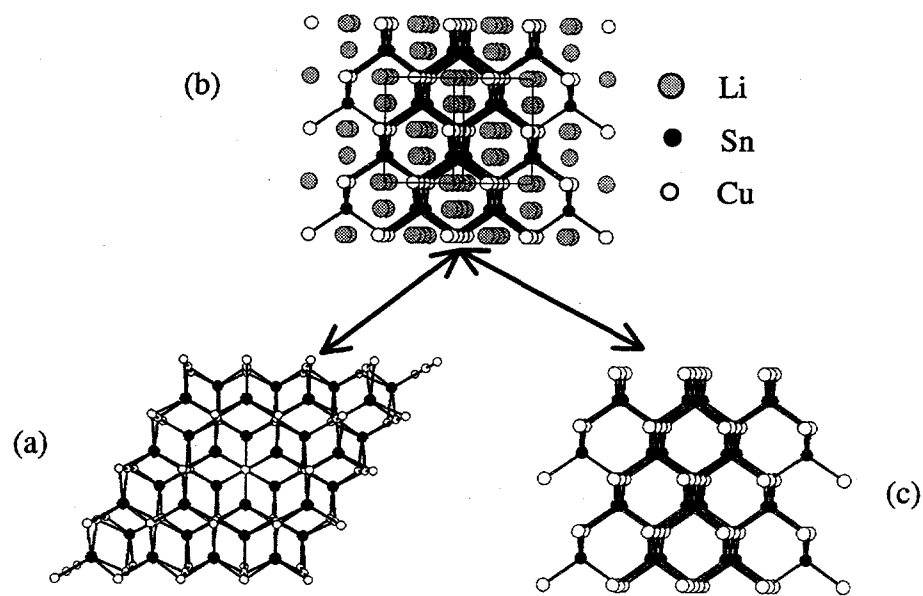


Figure 3